Journal of Zhejiang University SCIENCE A
ISSN 1673-565X (Print); ISSN 1862-1775 (Online)
www.zju.edu.cn/jzus; www.springerlink.com
E-mail: jzus@zju.edu.cn

Hysteresis model of magnetostrictive actuators and its numerical realization*

TANG Zhi-feng†, LV Fu-zai, XIANG Zhan-qin
(*Modern Manufacture Engineering Institute, Zhejiang University, Hangzhou 310027, China*)
†E-mail: tangzf2001@yahoo.com
Received Mar. 1, 2007; revision accepted Apr. 19, 2007

Abstract: This paper presents two numerical realization of Preisach model by Density Function Method (DFM) and *F* Function Method (FFM) for a giant magnetostrictive actuator (GMA). Experiment and simulation showed that FFM is better than DFM for predicting precision of hysteresis loops. Lagrange bilinear interpolation algorithm is used in Preisach numerical realization to enhance prediction performance. A set of hysteresis loops and higher order reversal curves are predicted and experimentally verified. The good agreement between the measured and predicted curves shows that the classical Preisach model is effective for modelling the quasi-static hysteresis of the GMA.

Key words: Magnetostrictive, Actuator, Hysteresis, Density Function Method (DFM), *F* Function Method (FFM)
doi:10.1631/jzus.2007.A1059 **Document code:** A **CLC number:** TH113; TH161

INTRODUCTION

Giant magnetostrictive actuators (GMAs) have advantages of solid state actuation, powerful force, fast response, high precision and have been applied in many fields such as vibration control, machine tool micro-positioning and fluid control. But it is well known that GMA has hysteresis, a form of non-negligible memory behavior, and mixes dynamic and rate-dependent memory effects together. Jile-Atherton model (Sablik and Jiles, 1988; Marcelo *et al*., 2000) and Preisach model (Smith, 1997; Chen *et al*., 2006) are the typical two methods that describe the GMA hysteresis. The Preisach model is a phenomenological hysteresis model that offers mathematical generality, and classical Preisach model is universally the most known to describe rate-independent hysteresis quite satisfactorily with acceptable computational cost (Davino *et al*., 2005). Some new modified Preisach model developed from classical Preisach for taking dynamic effects into account or describing high order hysteresis, such as moving Preisach model (Della Torre, 1990), modified generalized Preisach model (Mayergoyz and Frienman, 1988) and dynamic hysteresis model (Bernard and Mendes, 2002). But they suffer from heavy computation cost that makes them hard for practical application. Therefore this paper keeps on aiming at the classical Preisach model. Density Function Method (DFM) and *F* Function Method (FFM) are used for Preisach numerical implementation. Simulation and experimental results of the two methods are compared and discussed.

* Project supported by the National Natural Science Foundation of China (No. 50105019) and China Postdoctoral Science Foundation (No. 20060390337)

PREISACH MODEL AND ITS NUMERICAL REALIZATION

The classical Preisach model can be written as (Tan *et al*., 2001)

$$f(t)=\iint_{\alpha\geq\beta}\mu(\alpha,\beta)\hat{\gamma}_{\alpha\beta}[u(t)]\mathrm{d}\alpha\mathrm{d}\beta, \quad (1)$$

where $f(t)$ is the system output, $\mu(\alpha,\beta)$ is a density function or weighting function, $\hat{\gamma}_{\alpha\beta}[u(t)]$ is the hysteresis operator with output of 0 or +1, since the input current to GMA always exceeds zero, and α and β correspond to "up" and "down" switching values of the input $u(t)$, respectively.

DFM

DFM is based on the definition of the classical Preisach model, i.e. Eq.(1), with the discrete expression being

$$f(t)=\sum_{i=1}^{N}\mu_i A_i \hat{\gamma}_i[u(t)], \tag{2}$$

where A_i is the area of the ith discrete region. Fig.1a is the schematic drawing of the Preisach plane discretization where N=15. If the discrete cell is dense enough, the density function can be regarded as the same value in a discrete cell, and the hysteresis operator is also the same in the same cell. Therefore the exclusive unknown parameter in Eq.(2) is the density function μ_i.

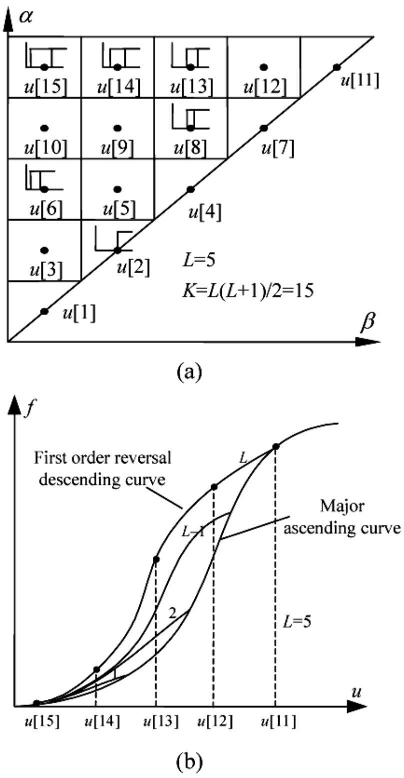

Fig.1 Discretization of Preisach plane. (a) Preisach plane; (b) The discretization points on the reversal descending curve

Some identification techniques are presented in (Gorbet and Wang, 1998; Natale and Velardi, 2001). However, measuring the major hysteresis loop and the first order reversal curves (Fig.1b) is necessary. The difference of identification is the method of the treating experimental data.

FFM

FFM is based on the pattern interpretation of the Preisach plane, which was proposed by Doong and Mayergoyz (1985) and Ge and Jouaneh (1995) for piezoelectric hysteresis model. Fig.2a is the schematic drawing of first order and second order reversal decreasing curves. The notation f_α is the output value on the limiting ascending branch corresponding to the input $u=\alpha$. The notation $f_{\alpha\beta}$ is the output value on the reversal curve attached to the limiting ascending branch at the point f_α. The output value corresponds to the input $u=\beta$.

Defining F function as:

$$F(\alpha,\beta)=(f_\alpha - f_{\alpha\beta}). \tag{3}$$

Fig.2b is the geometrical interpretation of F function in the Preisach plane. It is easy to prove that:

$$F(\alpha,\beta)=\iint_{T(\alpha,\beta)}\mu(x,y)\mathrm{d}x\mathrm{d}y. \tag{4}$$

$T(\alpha,\beta)$ is the triangle area in the Preisach plane.

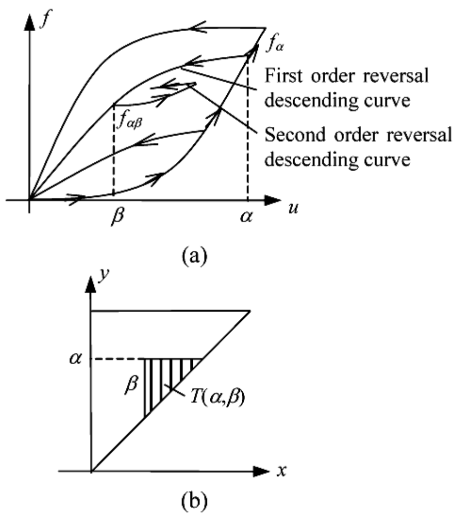

Fig.2 Geometrical interpretation of F function. (a) First and second order reversal descending curve; (b) The formation of triangle region in Preisach plane

A staircase curve forms with the variation of the input value. It separates the Preisach plane into two regions: $T_+(t)$ and $T_-(t)$ as shown in Fig.3.

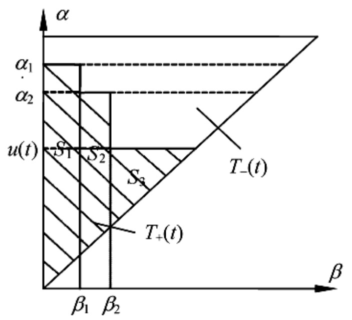

Fig.3 Memory curve separates the Preisach plane

From (Doong and Mayergoyz, 1985; Ge and Jouaneh, 1995), the numerical expressions of the classical Preisach model, for situations in which the last variation of the input is decreasing or increasing, can be written, respectively, as

$$f(t)=\sum_{k=1}^{N}\{[F(\alpha_k,\beta_{k-1})-F(\alpha_k,\beta_k)]+F(u(t),\beta_k)\},\quad \text{increasing}, \tag{5}$$

$$f(t)=\sum_{k=1}^{N-1}[F(\alpha_k,\beta_{k-1})-F(\alpha_k,\beta_k)]+[F(\alpha_N,\beta_{N-1})-F(\alpha_N,u(t))],\quad \text{decreasing}. \tag{6}$$

Therefore, if the F function sequence is known, the hysteresis output can be calculated.

EXPERIMENTS AND DISCUSSION

Experimental setup

An experimental test system depicted in Fig.4 was set up. The GMA developed by ourselves is presented in (Tang, 2005). An LVDT sensor (MHR010) is used to measure the displacement of the GMA. All signals are connected to the multifunction data acquisition device (DAQ, PXI6071E) installed in the NI frame (PXI1031). The measuring software is programmed in LabVIEW environment. The linear power amplifier is LVC5050 made by AETechron Corporation.

DFM and FFM both need the experimental data of first order reversal curves, so first a series of first-order reversal curves is tested for the GMA system of Fig.4. The input current has sinusoidal waveform, amplitude is greater than zero to avoid effect of twice the drive frequency, and the drive frequency is much less than the natural frequency of the system (Fig.5). Thus, these curves can be regarded as static hysteresis loops and therefore the classical Preisach model can be used. From Fig.6, it can be seen that the ascending curves almost coincide, giving rise to a major ascending curve. It can also be observed that $f_{\alpha\beta}$ monotonically increases with respect to α and β.

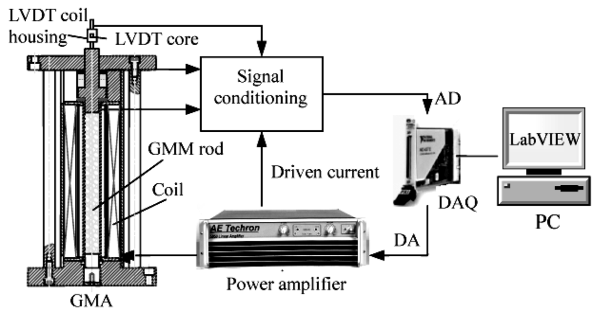

Fig.4 Schematic drawing of the experimental system

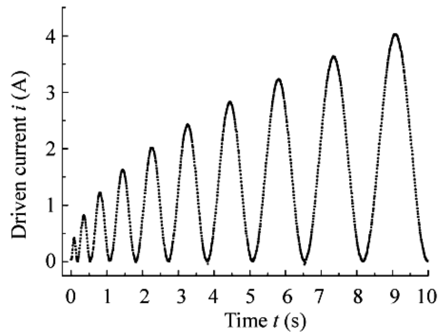

Fig.5 Input current signals

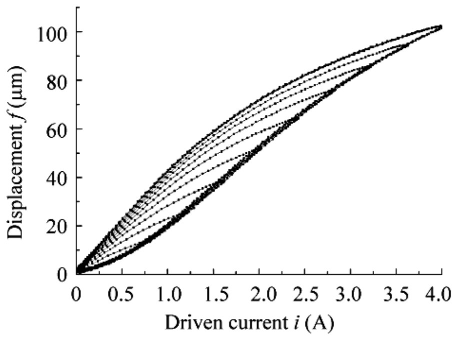

Fig.6 First order reversal descending curves

Parameter identification

Once first order reversal curves are measured, F function sequence is also known, which means the

Preisach numerical model is realized. But for DFM, there is one unknown parameter μ_i that needs to be identified.

Suppose the input current sequence is $\{u[i]\}_{i=1}^{K}$, and the measured displacement sequence is $\{\tilde{f}[i]\}_{i=1}^{K}$. The predicted displacement of the GMA is:

$$f[i]=\sum_{k=1}^{K}\mu_k A_k \hat{\gamma}_k[i],\ i=1,2,...,K; K=L(L+1)/2. \quad (7)$$

In Eq.(7), A_k is the area of the kth discrete region in the Preisach plane, and $\hat{\gamma}_k[i]$ is the Preisach operator that corresponds to the input $u[i]$. The density function μ is greater than zero since the displacement always exceeds zero. We use the least squares method to estimate the parameters:

$$\min\left\|\boldsymbol{CA\mu}-\tilde{\boldsymbol{f}}\right\|^2 \quad \text{s.t.}\ \ \boldsymbol{\mu}\geq 0, \quad (8)$$

where,

$$\boldsymbol{C}=\begin{bmatrix}\hat{\gamma}_1[1] & \hat{\gamma}_2[1] & \dots & \hat{\gamma}_K[1]\\ \hat{\gamma}_1[2] & \hat{\gamma}_2[2] & \dots & \hat{\gamma}_K[2]\\ \cdot & & & \cdot\\ \cdot & & & \cdot\\ \hat{\gamma}_1[N] & \hat{\gamma}_2[N] & \dots & \hat{\gamma}_K[N]\end{bmatrix}_{N\times K},$$

$$\boldsymbol{A}=\begin{bmatrix}A_1 & 0 & \cdot & \cdot & \cdot & 0\\ 0 & A_2 & & & & \cdot\\ \cdot & & \cdot & & & \cdot\\ \cdot & & & \cdot & & \cdot\\ \cdot & & & & \cdot & 0\\ 0 & \cdot & \cdot & \cdot & 0 & A_K\end{bmatrix}_{K\times K},$$

$$\boldsymbol{\mu}=[\mu_1\ \ \mu_2\ \ \dots\ \ \mu_K]',\quad \tilde{\boldsymbol{f}}=[\tilde{f}[1]\ \tilde{f}[2]\ \dots\ \tilde{f}[N]]'.$$

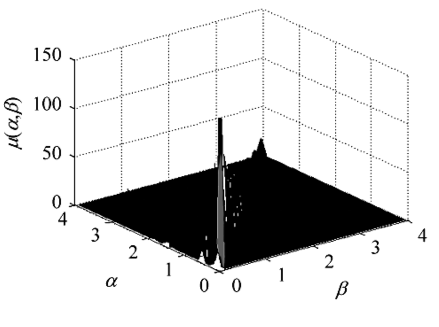

Fig.7 Distribution of the identified density function mass

Eq.(8) is a typical non-negative restriction least squares issue. We programmed in Matlab to solve the equation using the "lsqnonnegs" command. Fig.7 shows the distribution of the identified density function masses. It reveals that density function in many discrete cells equal zero, which means it could save much more memory space.

Prediction experiment

DFM and FFM are implemented to compare their prediction performance. Figs.8 and 9 are the tracking prediction and test results of DFM and FFM without interpolation algorithm. The input current has sinusoidal waveform, varying from 0~2 A, and a period of 1 s.

Theoretically, DFM and FFM should have the same accuracy based on the same experimental data. But it is revealed from Figs.8 and 9 that FFM has higher accuracy than DFM. We think it may be caused by the fact that the discretization level of 10 is not enough. It brings errors inevitably since density function is taken as the same value in a discrete cell, and parameter identification error is also unavoidable in DFM. But in FFM, errors just occurred in the regions near memory curves, so we choose FFM as our next study of 2D interpolation.

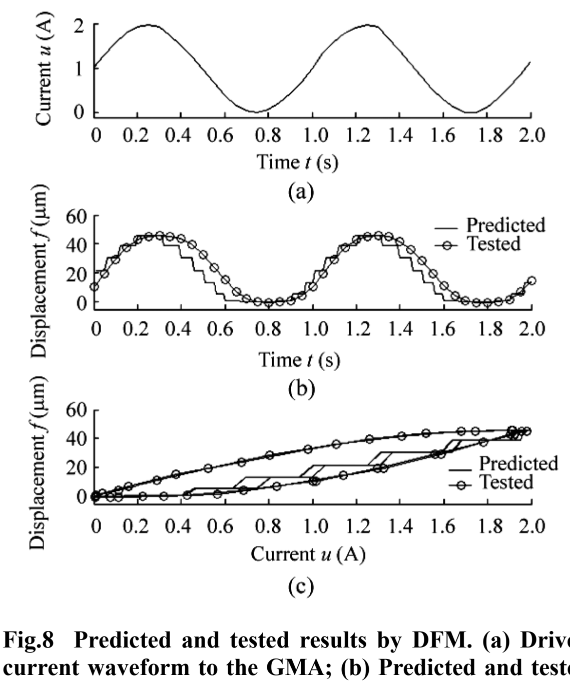

Fig.8 Predicted and tested results by DFM. (a) Driven current waveform to the GMA; (b) Predicted and tested displacement waveform by DFM; (c) Predicted and tested hysteresis loop by DFM

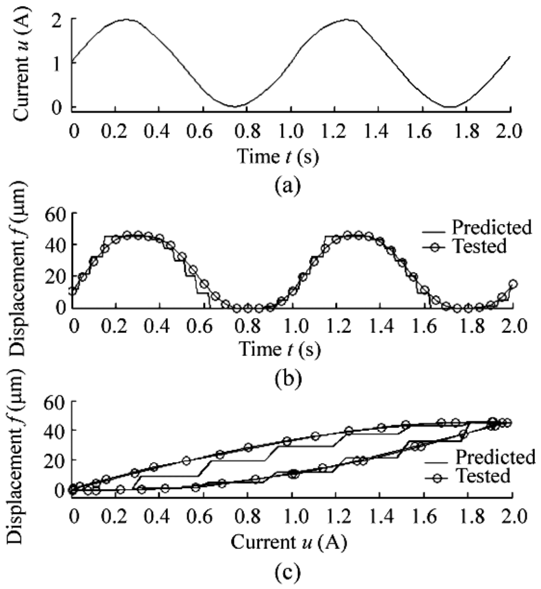

Fig.9 Predicted and tested results by FFM. (a) Driven current waveform to the GMA; (b) Predicted and tested displacement waveform by FFM; (c) Predicted and tested hysteresis loop by FFM

Lagrange bilinear interpolation is used to enhance prediction performance. If the vertices (α,β) fall in the quadrangle cell shown in Fig.10b, the F function value of the point can be expressed as:

$$F(\alpha,\beta)=N_1F(\alpha_i,\beta_j)+N_2F(\alpha_i,\beta_{j+1}) +N_3F(\alpha_{i+1},\beta_{j+1})+N_4F(\alpha_{i+1},\beta_j). \quad (9)$$

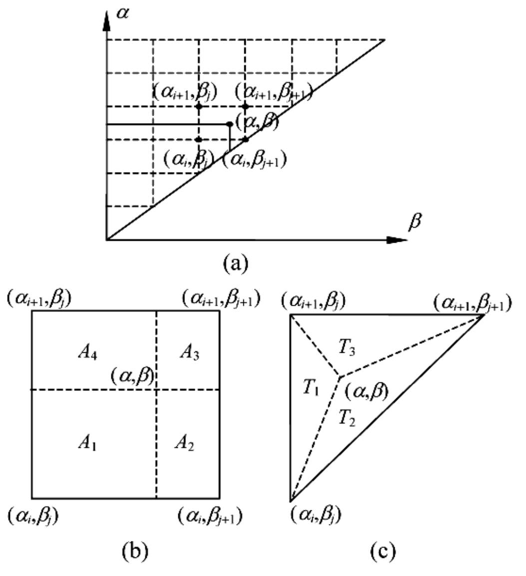

Fig.10 Illustration of 2D interpolation. (a) The big triangle region in Preisach plane; (b) The point drop in the rectangle region; (c) The point drop in the triangle region

The coefficient in Eq.(9) is defined as: $N_1=A_3/A$, $N_2=A_4/A$, $N_3=A_1/A$, $N_4=A_2/A$. A is the area of the discrete quadrangle cell. A_1, A_2, A_3, A_4 are the areas of the region separated by the vertices (α,β) respectively. If the vertices (α,β) fall in the triangle cell as shown Fig.10c, the F function value of the point can be expressed as:

$$F(\alpha,\beta)=\lambda_1F(\alpha_i,\beta_j)+\lambda_2F(\alpha_{i+1},\beta_j)+\lambda_3F(\alpha_{i+1},\beta_{j+1}). \quad (10)$$

The coefficient in Eq.(10) is defined as: $\lambda_1=T_3/T$, $\lambda_2=T_2/T$, $\lambda_3=T_1/T$. T is the area of the triangle cell, and T_1, T_2, T_3 are the areas of the separated region by the vertices (α,β) respectively. The coefficient can be calculated as (Shen and Liang, 1992):

$$\begin{cases}1=\lambda_1+\lambda_2+\lambda_3,\\ \alpha=\lambda_1\alpha_i+\lambda_2\alpha_{i+1}+\lambda_3\alpha_{i+1},\\ \beta=\lambda_1\beta_j+\lambda_2\beta_j+\lambda_3\beta_{j+1}.\end{cases} \quad (11)$$

For a sinusoidal input signal, varying from 0 to 3 A, frequency of 1 Hz, the hysteresis loop predicted by the F function realization using interpolation algorithm and the experimental loop are compared in Fig.11. It can be seen that they match each other well. The error of predicted path under different driven current variation (sinusoidal waveform, frequency 1 Hz) is given in Table 1.

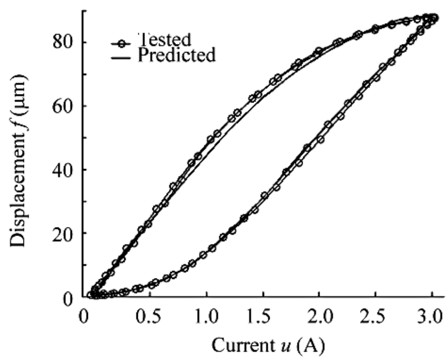

Fig.11 Predicted and tested result by interpolation algorithm

Table 1 shows that the predicted error increases with driven current increases. This accords with the fact that the non-linearity intensifies with the increase of driven current. More densely discretization in the severe non-linearity region can keep the predicted error stable. Application of nonuniform discretization technique to Preisach numerical realization is our ongoing study work.

Table 1 Predicted error for different current variation

u (A)	f (μm)	e_{max} (μm)	r (%)
0~1	0~13	0.5	3.8
0~2	0~45	2.0	4.4
0~3	0~88	4.5	5.1
0~4	0~107	7.5	7.0

u: current; f: displacement; e_{max}: maximum error; r: error ratio

The predicted GMA higher order hysteresis curves were verified experimentally and the results are compared in Fig.12. The close match between the simulated curve and the experimental curve shows that the classical Preisach model works well for simulating higher order hysteresis curves for low-frequency input signals.

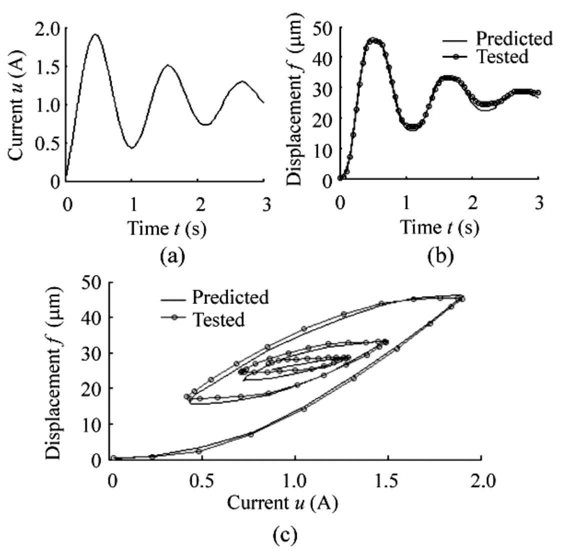

Fig.12 Predicted and tested result of high order curves. (a) Variation of the driven current's amplitude; (b) Predicted and tested displacement waveform; (c) Predicted and tested high order hysteresis loop

CONCLUSION

This paper presents Preisach modelling of hysteresis of a GMA by two numerical realization: DFM and FFM. To implement the numerical model, a set of first-order hysteretic reversal curves is measured. Experiment and simulation show that FFM is better than DFM over predict precision of hysteresis loops. Lagrange bilinear interpolation algorithm is used in FFM to enhance prediction performance. A set of hysteresis loops and higher order reversal curves are predicted based on experimental data and experimentally verified. The predicted error is acceptable and it increases with the input current increases. Prediction experiment verified that the classical Preisach model is effective for modelling the hysteresis of the GMA under low-frequency input current.

References

Bernard, Y., Mendes, E., 2002. Dynamic hysteresis modeling based on Preisach model. *IEEE Transaction on Magnetics*, **38**(2):885-888. [doi:10.1109/20.996228]

Chen, Z.Q, Guo, C., Zhao, J.X., 2006. Modeling and control of hysteretic systems based on Preisach model. *Control Engineering of China*, **4**:304-306.

Davino, D., Natale, C., Pirozzi, S., 2005. A fast compensation algorithm for real-time control of magnetostrictive actuators. *Journal of Magnetism and Magnetic Materials*, **290-291**:1351-1354. [doi:10.1016/j.jmmm.2004.11.435]

Della Torre, E., 1990. Preisach modeling and reversible magnetization. *IEEE Transactions on Magnetics*, **26**(6):3052-3058. [doi:10.1109/20.102890]

Doong, T., Mayergoyz, I.D., 1985. On numerical implementation of hysteresis models. *IEEE Transactions on Magnetics*, **21**(5):1853-1855. [doi:10.1109/TMAG.1985.1063923]

Ge, P., Jouaneh, M., 1995. Modeling hysteresis in piezoceramic actuators. *Precision Eng.*, **17**(3):211-221. [doi:10.1016/0141-6359(95)00002-U]

Gorbet, R.B., Wang, D.W.L., 1998. Preisach Model Identification of a Two-Wire SMA Actuator. Proceedings of the 1998 IEEE International Conference on Robotics & Automation, Leuven, Belgium, **5**:2161-2167.

Marcelo, J.D., Ralph, C.S., Alison, B.F., 2000. Structural magnetic strain model for magnetostrictive transducers. *IEEE Transactions on Magnetics*, **3**:545-556.

Mayergoyz, I.D., Frienman, G., 1988. Generalized Preisach model of hysteresis (invited). *IEEE Transactions on Magnetics*, **24**(1):212-217. [doi:10.1109/20.43892]

Natale, C., Velardi, F., 2001. Modelling and Compensation of Hysteresis for Magnetostrictive Actuators. 2001 IEEE/ASME International Conference on Advanced Intelligent Mechatronics, Como, Italy, **5**:744-749.

Sablik, M.J., Jiles, D.C., 1988. A model for hysteresis in magnetostriction. *J. Appl. Phys.*, **64**(10):5402-5404. [doi:10.1063/1.342383]

Shen, Y.H., Liang, Z.H., 1992. Handbook of Applied Mathematics. Science Press, Beijing (in Chinese).

Smith, R.C., 1997. Modeling techniques for magnetostrictive actuators. *Proceedings of SPIE*, **3041**:243-253. [doi:10.1117/12.275690]

Tan, X.B., Venkataraman, R., Krishnaprasad, P.S., 2001. Control of hysteresis: Theory and experimental results. *Proceedings of SPIE*, **4326**:101-112. [doi:10.1117/12.436463]

Tang, Z.F., 2005. Fundamental Theory and Experiments Study of Giant Magnetostrictive Actuator. Ph.D Thesis, Zhejiang University, Hangzhou (in Chinese).